Vibration Suppression of Handling Robot with Timing Belts Based on Two-mass Model

Bulletin of University of Osaka Prefecture
Vol. 41, No. 2, 1993, pp. 1−11.

Vibration Suppression of Handling Robot with Timing Belts Based on Two-mass Model

Shigeo MORIMOTO*, Koichi FUKADA**, Yoji TAKEDA*
and Takao HIRASA*

(Received Oct. 31. 1992)

A robot arm with timing belts is modeled in this paper with consideration given to this flexibility, and the appropriateness of the proposed mechanical model is examined based on computer simulations and experimental results. A positioning servo system using state feedback to suppress vibrations based on this mechanical model is also presented. The performance of the proposed control system and the effect of the suppression of vibrations are also examined based on the computer simulations and experimental results.

1. Introduction

Timing belts have been widely used in many industrial applications due to such advantages as no backlash. When a timing belt is used in a robot arm, however, it is difficult to drive the arm without vibrations due to the flexibility of the belt. It follows that these vibrations must be eliminated in order to obtain a mechanical system with smooth motion. These vibrations can be eliminated if the poles of the system are placed away from the imaginary axis[1−3]. To examine the poles of the system, the model of the robot arm with transmission elasticity as well as the model of the actuator is needed.

This paper presents the modeling of the robot arm with the timing belts and the vibration suppression by using the linear state feedback theory. The model of the robot is derived from the Lagrangian equations and the transmission elasticity is approximated to a torsional spring. The proposed control system is realized with a software servo system using 80286 and 80287 microprocessors as the positioning servo and vibration suppression control system.

* Department of Electrical Engineering, college of Engineering
** Graduate Student, Department of Electrical Engineering, College of Engineering

2. Modeling

A. Dynamic Model

The robot arm used in these studies is shown in Fig. 1. A DC motor is connected to a joint 1 through a harmonic drive gear as an actuator. The timing belts are provided between joints 1, 2 and 3 to drive link 3 along the X axis. In this model the flexibility of the timing belts produces vibrations in primarily joint 2.

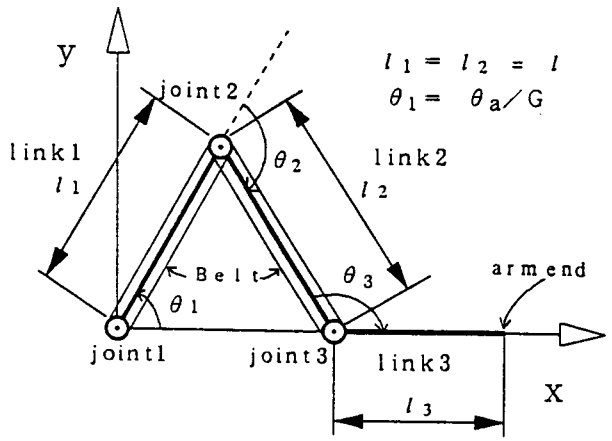

Fig. 1 Schematic of the robot with the timing belts.

The dynamic equation for a robot arm based on Lagrangian formulation can be described as follows[4]:

$$\tau_1 = M_1(\theta_1)\ddot{\theta}_1 + H_1(\theta_1, \dot{\theta}_1) + V_1\dot{\theta}_1 + \tau_{cl} \tag{1a}$$

$$M_1(\theta_1) = m_1(\theta_1) + m_2(\theta_1) + m_3(\theta_1) \tag{1b}$$

where $M_1(\theta_1)$ is the total moment of inertia for the arm, $m_1(\theta_1)$, $m_2(\theta_1)$, $m_3(\theta_1)$ are the moment of inertia for link 1, link 2 and link 3, $H_1(\theta_1, \dot{\theta}_1)$, V_1 are the Corioris and centrifugal forces, the viscous friction coefficient respectively, θ_1, $\dot{\theta}_1$ and $\ddot{\theta}_1$ are the joint angular position, velocity, and acceleration respectively, and τ_1, τ_{cl} are the joint torque, coulomb friction respectively.

In order to implement proper control algorithms, the above dynamic equation for a robot arm should be converted to the equivalent dynamics with respect to an actuator. The dynamic equation for an actuator can be described as follows:

$$\tau_m = M_a\ddot{\theta}_a + V_a\dot{\theta}_a + \tau_a + \tau_{ca} \tag{2}$$

where M_a, V_a are the total moment of inertia and the viscous friction coeffi-

cient of the actuator respectively, $\dot{\theta}_a$, $\ddot{\theta}_a$ are the actuator shaft velocity and acceleration, τ_m, τ_a and τ_{ca} are the driving torque, the transmission torque to the links and the coulomb friction respectively.

Due to the large gear reduction ($G=88$) of this robot arm, the joint torque $\tau_1(=G\tau_a)$ at the actuator shaft is reduced by the gear ratio G. Therefore, the interactions of nonlinearity and coupling effects of the links are largely reduced and negligible, and the drive system tends to dominate the dynamics at the actuator shaft. Therefore, the arm-actuator dynamics at the actuator shaft can be described by the following equation :

$$\tau_m=[M_a+M_g+M_1(\theta_1)/G^2]\ddot{\theta}_a+V_{al}\dot{\theta}_a+\tau_c \tag{3}$$

where relationship between the actuator shaft angle θ_a and the robot link joint angle θ_1 is $\theta_a=G\theta_1$, M_g is the inertia of the harmonic drive gear, V_{a1} is the corresponding viscous friction coefficient, and τ_c is the total coulomb friction at the actuator shaft.

B. Torsional Model

Some undesirable vibrations occur during operation due to the flexibility of the timing belts in primarily joint 2. This is caused by transmission elasticity between link 1 and link 2. Therefore the robot arm with transmission elasticity is modeled approximately in Fig. 2[1-3),5)].

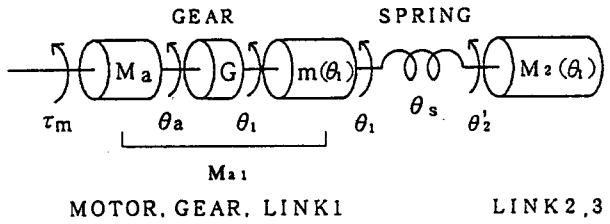

Fig. 2 Model of a robot arm with transmission elasticity.

The transmission elasticity is approximated to a torsional spring and the inertia for link 2, 3 connected with the transmission end is given in (4) below.

$$M_2=m_2(\theta_1)+m_3(\theta_1) \tag{4}$$

Thus, an approximated mechanical model for the dynamics of this robot, specifically a robot driven by a DC motor and exhibiting flexibility in the timing belts, is given in (5) below.

$$\tau_m=M_{a1}\ddot{\theta}_a+V_{a1}\dot{\theta}_a+\tau_c+K_s(\theta_1-\theta'_2)/G \tag{5a}$$
$$(M_2/G)\ddot{\theta}'_2=K_s(\theta_1-\theta'_2)/G \tag{5b}$$

where K_s is the spring constant of the belt, $\theta'_2(\theta_2/2$ in Fig. 1) is the joint angular position including the torsion. From (5a) and (5b), the mechanism of this robot with transmission elasticity can be approximated to the two mass systems. A block diagram of the mechanical system based on (5a) and (5b) is shown in Fig. 3.

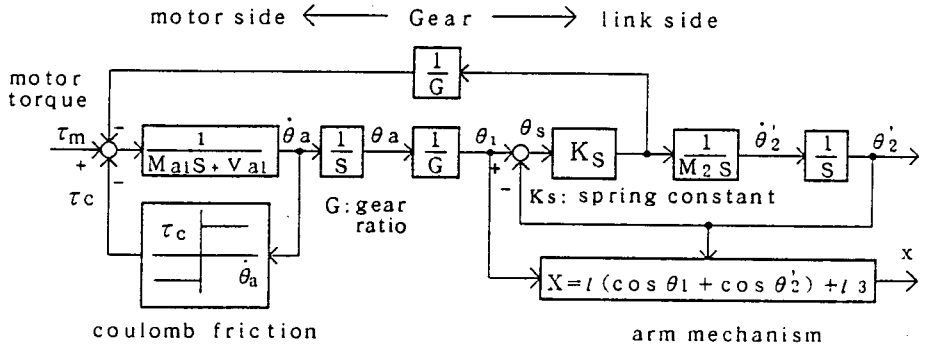

Fig. 3 Block diagram of the mechanical system.

The position of the robot arm end is given by a coordinate transformation from the motor space to a task space. The experimental responses of the velocity, acceleration of the robot arm, and the motor velocity are shown in Fig. 4(a), in which the trapezoidal curve is given as the reference of the motor velocity. (The position of the robot arm end is expressed by r, where $r=2l+l_3-x$.) The motor velocity $\dot{\theta}_a$ shows good response according to the reference with no vibrations. Significant vibrations are noticed at the arm end due to the flexibility of the timing belts.

Table 1 Parameters of the robot arm

l	0.25	m
M_{a1}	0.000063	kg•m²
V_{a1}	0.00035	N•m•s/rad
τ_c	0.032	N•m
$M_2(\theta_1=0$[deg])	0.01	kg•m²
K_s	33	N•m/rad

The results of computer simulations based on the block diagram in Fig. 3 are shown in Fig. 4(b) under the same condition shown in Fig. 4(a). We can conclude from Fig. 4(a) and 4(b) that the mechanical model of this robot designed with consideration for the flexibility of the timing belts accurately represents the real system.

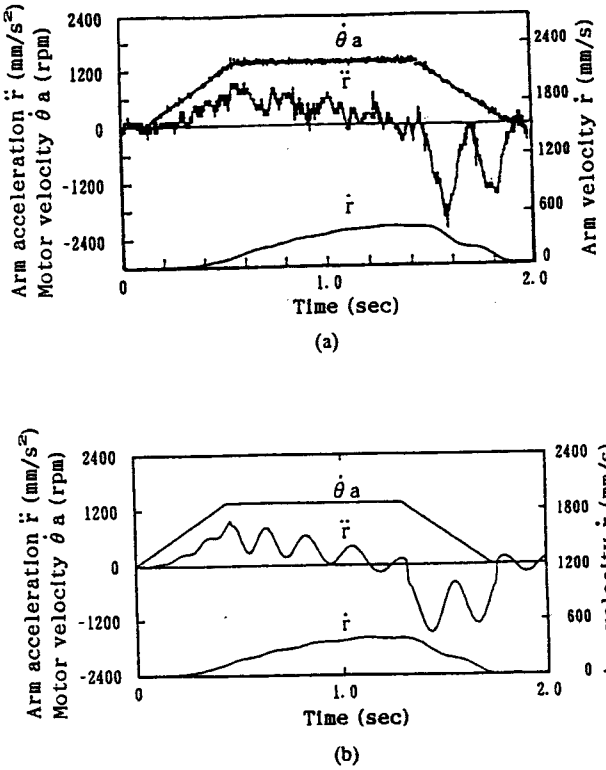

Fig. 4 Response of the robot arm in the mechanical system.
(a) Experiment. (b) Simulation.

3. Suppression of Vibrations

A linear state feedback was therefore introduced to this system as a means of reducing vibrations[1-3].
Equations (5a) and (5b) are thus rewritten as

$$\dot{x}=Ax+bu \tag{6a}$$
$$y=cx \tag{6b}$$

where

$$x=[\theta_a \dot{\theta}_a \theta_s \dot{\theta}_s]^T \tag{6c}$$

$$A=\begin{bmatrix} 0 & 1 & 0 & 0 \\ 0 & -\frac{V_{al}}{M_{al}} & -\frac{K_s}{M_{al}G} & 0 \\ 0 & 0 & 0 & 1 \\ 0 & -\frac{V_{al}}{M_{al}G} & -K_s\left(\frac{1}{M_{al}G^2}+\frac{1}{M_2}\right) & \end{bmatrix} \tag{6d}$$

$$b=\begin{bmatrix} 0 & \frac{1}{M_{al}} & 0 & -\frac{1}{M_{al}G} \end{bmatrix}^T \tag{6e}$$

$$c=\begin{bmatrix} 1 & 0 & 0 & 0 \\ 0 & 1 & 0 & 0 \end{bmatrix} \tag{6f}$$

$$\theta_s=\frac{\theta_a}{G}-\theta'_2. \tag{6g}$$

It should be noted that coulomb friction τ_c is neglected in this state. It is difficult to reduce the vibrations of the mechanical system if only the valuables of state θ_a and $\dot{\theta}_a$ at the actuator are given as feedback valuables. This is caused by increasing of the order of the controlled system due to the tansmission elasticity. This vibration problem can be solved by giving all valuables of state in (6c) on the assumption that all valuables of state can be detected. In these studies, however, only torsional velocity $\dot{\theta}_s(=\dot{\theta}_1-\dot{\theta}'_2)$ is given as a feedback valuable in order to simplify the control algorithm. Only one value $\dot{\theta}_s$ is enough to reduce the vibrations of the mechanical system. The poles of the system with the state feedback will be examined later.

The torque command τ^{cmd} is given as a feedforward term by calculating the reverse dynamics. Thus, the input u in the state form is defined as

$$u=-\boldsymbol{K}\boldsymbol{x}+\tau^{cmd} \tag{7a}$$

where

$$\boldsymbol{K}=[000K_4]. \tag{7b}$$

4. Position Servo Control System

This linear state feedback and feedforward system is expanded to a position servo control system[4),6-7)]. Fig.5 is a block diagram of a position servo control system with suppression of vibrations. A state feedback and a servo compensator are added to the mechanical system of the robot arm in Fig.3.

The feedforward term in (7a) is given using the computed torque method[4),6)], in

which the parameters of the motor dynamics are nominal values identified by the experiment. Therefore, the feedforward torque based on the dynamic model in (3) is given in (8a) and (8b) below.

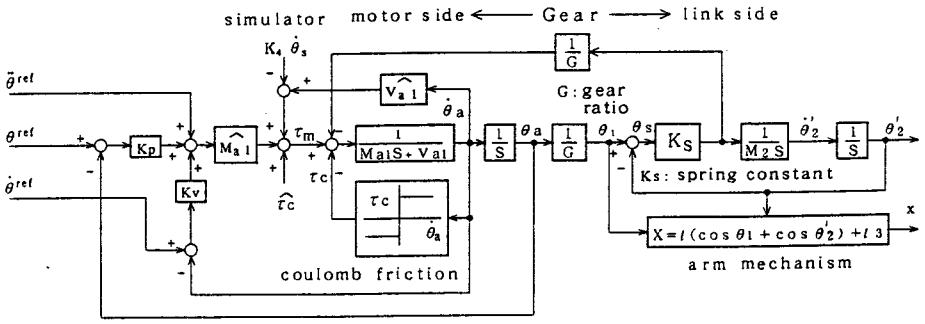

Fig. 5 Block diagram of the position servo control system.

$$\tau^{cmd}=\hat{M}_{al}u_1+\hat{V}_{al}\dot{\theta}_a+\hat{\tau}_c \tag{8a}$$

$$u_1=\ddot{\theta}_a^{ref} \tag{8b}$$

where $\hat{M}_{al}$, $\hat{V}_{al}$ and $\hat{\tau}_c$ are nominal values of M_{al}, V_{al} and τ_c respectively.

Since some tracking errors may be occur during operation due to the parameters variation of the model, a position servo compensator which consists of **PD** terms and a reference of the acceleration has to be added to this system. Thus u_1 in (8a), (8b) is rewritten as

$$u_1=\ddot{\theta}_a^{ref}+K_v(\dot{\theta}_a^{ref}-\dot{\theta}_a)+K_p(\theta_a^{ref}-\theta_a)\ . \tag{9}$$

The error equation is governed by

$$\ddot{e}+K_v\dot{e}+K_pe=0 \tag{10a}$$

where

$$e=\theta_a^{ref}-\theta_a. \tag{10b}$$

Then, if we choose **PD** gains such that the equation (10a) has negative roots, e approaches zero asymptotically. In this case, **PD** gains K_p, K_v are described as $K_p=\omega_n^2$, $K_v=2\xi\omega_n$, where ξ is a damping coefficient and ω_n is a natural frequency, and the response of the system is decided by ξ and ω_n. Therefore, the motor-driving torque τ_m which means the input u in a state form is defined as

$$\tau_m=\hat{M}_{al}u_1+\hat{V}_{al}\theta_a+\hat{\tau}_c-K_4\dot{\theta}_s. \tag{11}$$

The pole assignments of this system in Fig.5 are shown in Fig.6. Fig.6(a) in which the **PD** gains K_p, K_v are constant and a valuable parameter is K_4 shows that the dominant poles of this system are away from the imaginary axis as the state feedback gain K_4 is large and the system becomes non-vibration as the result. Besides Fig.6(a) shows that only the torsional velocity $\dot{\theta}_s$ is enough to reduce the vibrations of this system. From Fig.6(b) in which the state feedback gain K_4 and the damping coefficient ζ are constant in an appropriate value and parameter is ω_n, the gains K_p, K_v cannot be large values in terms of reduction of vibrations. These pole assignments are discussed under the condition such that the moment of inertia M_2 takes the value at $\theta_1=90$[deg].

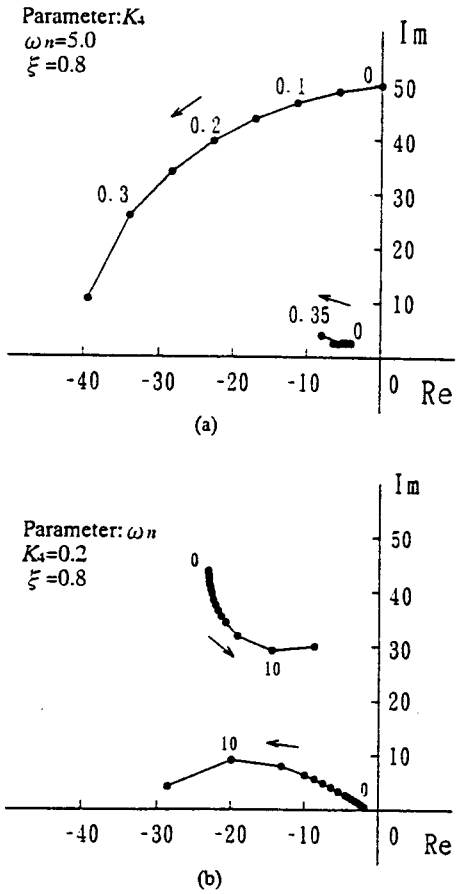

Fig. 6 Pole assignments of the proposed system for the parameters (a) K_4 and (b) ω_n.

5. Experimental Results

Table 2 Gain parameters in the experiment

K_4	0.15
K_p	25
K_v	20
ξ	2.0
ω_n	5.0

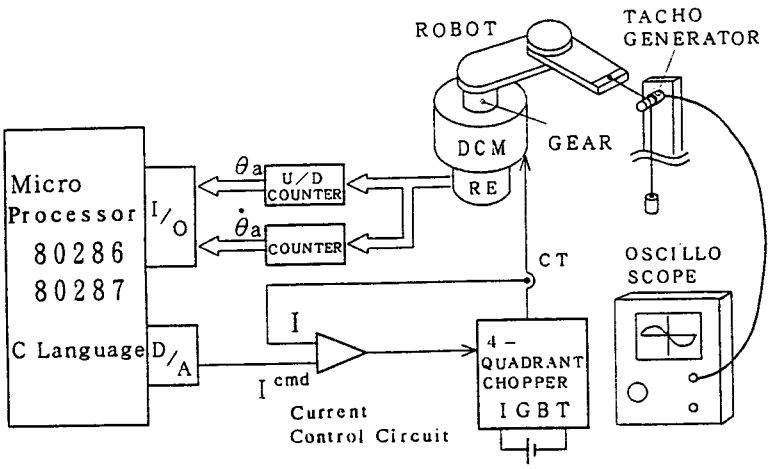

Fig. 7 Schematic of the experimental equipment.

The experimental results are examined by the control equipment in Fig. 7. This control system is realized with a software servo system using 80286 and 80287 microprocessors. The control algorithm is written in C language and the sampling time of this software servo control system is 1.5ms. The position θ_a and velocity $\dot{\theta}_a$ of the motor are detected by a rotary encoder and the torsional velocity $\dot{\theta}_s$ is calculated in software by a dynamic simulation of the robot arm. The velocity $\dot{r}$ of the robot arm end which moves linearly is measured by a tacho-generator as shown in Fig.7 and the acceleration $\ddot{r}$ of the robot arm end is obtained by differentiating the velocity $\dot{r}$. Gain parameters K_4, K_p, K_v are chosen based on the pole assignment in Fig. 6(a), 6(b), however, in order to enhance the stiffness of the servo system due to the parameters variation of the mechanical system, a damping coefficient ξ is comparatively large in the experimental system.

The experimental results and computer simulations are shown in Fig. 8(a) and

8(b). The characteristics of simulation results in Fig. 8(b) are appeared in the Fig. 8(a) and significant vibrations are reduced by the state feedback in comparison with Fig. 4(a).

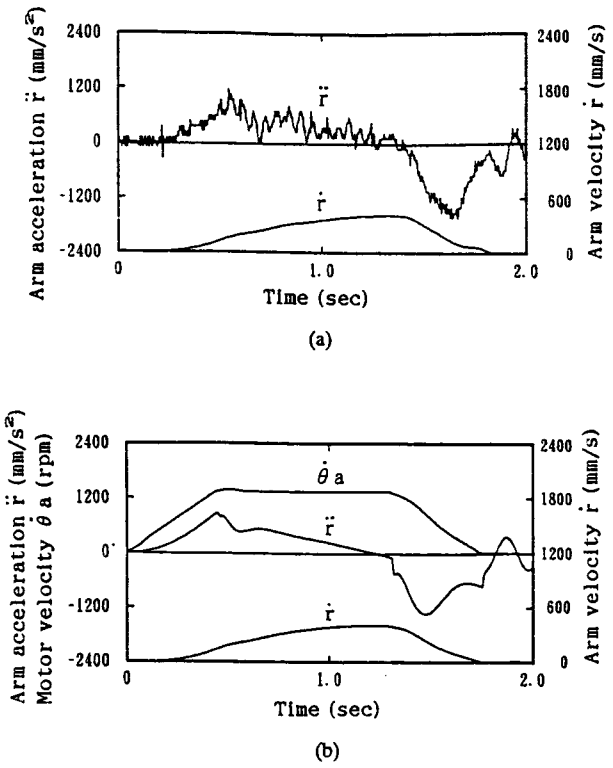

Fig. 8 Response of the robot arm in the position control system with supression of vibrations.
(a) Experiment (b) Simulation

6. Conclusion

This paper presented the position servo control system for the robot arm with timing belts. Based on the torsional model as well as the dynamic model of the robot arm, the linear state feedback theory is applied to the position control system to suppress the vibrations of the robot arm. The performance of the proposed control system and the effect of the suppression of vibrations were examined based on the computer simulations. This control system was implemented in the experimental system which was realized with a software servo system.

From the experimental results we could confirm that the proposed control system were effective to obtain the mechanical system with smooth motion.

References

1) T. Uno, S. Kudo, Y. Nishi, and T. Wada, "Control of Robot Arm with Software Servo System," T. IEE Japan, Vol.107-D, No.8, '87
2) S. Ouchi, K. Yano, "Control of Oscillating Multi-mass System with Gear Backlash by Digital Observer," T. IEE Japan, Vol.110-D, No.4, '90
3) J. Furusho, A. Sano, T. Sahashi, and H. Nagao, "Vibration Absorption Control of Robot Arm," JSME Japan, No.88-1159A
4) T. Yoshikawa, "Foundations of Robot Control," CORONA PUBLISHING CO, LTD.
5) J. Y. Hung, "Control of Industrial Robots that Have Transmission Elasticity," IEEE Trans. Industrial Electronics, Vol.38, No.6, Dec. 1991
6) K. Furuta, K. Kosuge, "Motion Control of Manipulators," T. IEE Japan, Vol.107-D, No1, '87
7) T. C. Steve Hsia, A. Lasky, and Z. Guo, "Robust Independent Joint controller Design for Industrial Robot Manipulators," IEEE Trans. Industrial Electronics, Vol.38, No.1, Feb. 1991